Research Repository UCD

| | |
|---|---|
| ***Title*** | Inertia considerations within unit commitment and economic dispatch for systems with high non-synchronous penetrations |
| ***Authors(s)*** | Daly, Pádraig, Flynn, Damian, Cunniffe, Noel |
| ***Publication date*** | 2015-07-02 |
| ***Publication information*** | Daly, Pádraig, Damian Flynn, and Noel Cunniffe. "Inertia Considerations within Unit Commitment and Economic Dispatch for Systems with High Non-Synchronous Penetrations." IEEE, July 2, 2015. https://doi.org/10.1109/ptc.2015.7232567. |
| ***Conference details*** | 2015 IEEE PowerTech, Eindhoven, Netherlands, 29 June - 2 July 2015 |
| ***Publisher*** | IEEE |
| ***Item record/more information*** | http://hdl.handle.net/10197/8090 |
| ***Publisher's statement*** | © 2015 IEEE. Personal use of this material is permitted. Permission from IEEE must be obtained for all other uses, in any current or future media, including reprinting/republishing this material for advertising or promotional purposes, creating new collective works, for resale or redistribution to servers or lists, or reuse of any copyrighted component of this work in other works. |
| ***Publisher's version (DOI)*** | 10.1109/ptc.2015.7232567 |

Downloaded 2026-05-01 23:36:30

The UCD community has made this article openly available. Please share how this access benefits you. Your story matters! (@ucd_oa)

© Some rights reserved. For more information

# Inertia Considerations within Unit Commitment and Economic Dispatch for Systems with High Non-Synchronous Penetrations

Pádraig Daly, Damian Flynn
Electricity Research Centre, University College Dublin
Dublin, Ireland
padraig.daly@ucdconnect.ie, damian.flynn@ucd.ie

Noel Cunniffe
EirGrid Plc
Dublin, Ireland
noel.cunniffe@eirgrid.com

***Abstract*—The priority dispatch status of non-synchronous renewable generation (wind, wave, solar), and increasing levels of installed high voltage direct current interconnection between synchronous systems, is fundamentally changing unit commitment and economic dispatch (UCED) schedules. Conventional synchronous plant, the traditional provider of services which ensure frequency stability - synchronising torque, synchronous inertia and governor response - are being displaced by marginally zero cost non-synchronous renewables. Such a trend has operational security implications, as systems - particularly synchronously isolated systems - may be subject to higher rates of change of frequency and more extreme frequency nadirs/zeniths following a system disturbance. This paper proposes UCED-based strategies to address potential shortfalls in synchronous inertia associated with high non-synchronous penetrations. The effectiveness of the day-ahead strategies is assessed by weighing the cost of the schedules against the risk level incurred (the initial rate of change of frequency following a generation-load imbalance), and the level of wind curtailment engendered.**

***Index Terms*—economic dispatch, inertia, unit commitment, wind generation.**

## I. Introduction

As countries attempt to reduce fossil fuel dependency and greenhouse gas emissions, penetration levels of renewable generation - most notably variable-speed wind turbines (VSWT) and solar photovoltaics (PV) - continue to rise. A fundamental difference with VSWT/PV generators, in comparison to conventional generation, is their non-synchronous connection to the power system, i.e. through partial/full-scale frequency converters. This decoupling of the VSWT rotor angular speed from the grid frequency results in there being no inherent change in stored rotational energy, and thus no inherent provision of an inertial response, to redress a falling/rising system frequency. The growth of high voltage direct current (HVDC) interconnection between synchronous systems has also accentuated the level of non-synchronous infeeds. Furthermore, the current electricity market environment - whereby the emphasis of conventional plant manufacturing is now focused on machine efficiency/flexibility [1] - is resulting in machines with lower inertial constants. Such trends are resulting in lower levels of synchronous inertia online, with a potential twofold impact on the system short-term frequency response: (i) the rate of change of frequency (ROCOF) following a generation-load imbalance is faster, which can result in (ii) more extreme nadirs/zeniths within a shorter time frame.

Traditionally, low levels of synchronous inertia were only of concern to smaller, synchronously isolated systems. However, the transition towards 'lighter' systems has been recognised in larger jurisdictions, such as in the U.S. [2], [3], continental Europe [4] and Great Britain [5]. Some system operators are already taking mitigating action: ERCOT [6] and EirGrid [7] are designing ancillary services to remunerate providers of synchronous inertia, and, along with Transpower [8], fast frequency response ($\leq$ 2 s full deployment). In contrast, Hydro-Québec have mandated an emulated inertial response capability from wind farms via grid code enforcement [9].

Conventional synchronous plant have been the cornerstone of power system frequency control, and consequently, operational policies have been based on the ubiquitous presence of such technology. Many of the challenges in managing a synchronous system with high installed capacities of non-synchronous renewable generation relate to the maximum allowable real-time penetration level of non-synchronous sources [10]. Limiting the instantaneous non-synchronous penetration to enhance system security has implications for renewable energy targets/economic system operation as it may result in wind curtailment [11], and may also incur start-up and production costs associated with committing and running out-of-merit synchronous plant [12]. Both consequences imply inefficient system operation. Thus, there is a pressing need to develop new operational policies, focused on the evolving plant portfolio - rather than those based on the unequivocal presence of conventional synchronous generation.

This work proposes unit commitment and economic dispatch (UCED)-based strategies to mitigate potential shortfalls

This work was conducted in the Electricity Research Centre, University College Dublin, Ireland, in collaboration with EirGrid Plc. The Electricity Research Centre is supported by the Commission for Energy Regulation, Bord Gáis Energy, Bord na Móna Energy, Cylon Controls, EirGrid, Electric Ireland, Energia, EPRI, ESB International, ESB Networks, Gaelectric, Intel, SSE Renewables, and UTRC. The work of Pádraig Daly was supported by the Irish Research Council's Embark Initiative.

in system inertia levels. A range of constraint and operational metric formulations are analysed, with focus placed on the initial ROCOF following a major event, system production costs, and wind curtailment.

## II. Inertial Constraint Formulation

### A. Short-Term Frequency Stability Time Frame

Short-term frequency control refers to the time frame immediately following a generation-load imbalance. There are three consecutive and distinct response stages [13]: (i) the proximity effect, (ii) the inertial response, and (iii) the governor response. Due to rotor inertia, synchronous machine rotor angles will not instantly change following a disturbance. The energy stored in the rotating masses cannot be immediately applied, and at the instant of an active power imbalance ($t = 0^+$), the energy supplied by the online generators comes from the energy stored in their magnetic field. The proximity effect is a purely electrical response [14], and is exclusive to synchronous generation, regardless of apparent power rating.

The inertial time frame follows the proximity effect. Its initiation will vary with system size, but is typically of the order of 1 or 2 s. The inertial time frame corresponds to when all online machines experience the same mean deceleration/acceleration following the loss of generation/load, i.e. synchronising swings have occurred. During the inertial time frame, the energy supplied by synchronously-connected machines comes from the energy stored due to their rotational motion.

When a frequency deviation exceeds a certain limit (the governor deadband), turbine-governor control will be activated. The governor response ensures rotor accelerations eventually become zero, and a new steady-state is reached. Unlike the inherent proximity effect and inertial response, the governor response requires control action.

### B. Inertial Constraint Implementation within UCED

The dynamic motion of a conventional unit's rotor is determined by the swing equation - a nonlinear second-order differential equation, with the 'complete' set of system equations including $N$ (the number of online units) swing equations coupled via the algebraic network equations. However, frequency stability *is determined by overall response of the system as evidenced by its mean frequency, rather than the relative motion of machines* [15]. Thus, frequency stability analysis concentrates on the overall system stability for sudden changes in generation-load balance, as opposed to machine stability. The 'complete' model can be simplified to a single linear first-order differential equation, Eq. (1) [16], and if used appropriately, this single bus frequency model can estimate the essential characteristics of a synchronously isolated system's frequency response [17], [18]. In the context of day-ahead optimisation of operational cost and security, the single bus frequency representation was deemed adequate, particularly considering transmission system operator requirements for computationally efficient UCED simulations, due to time constraints of control room operation.

Applied to the inertial time frame, i.e. well before initiation of the governor response, $t_{gov}$, the single bus frequency model is a system-level representation of how an active power imbalance is absorbed by the system. Should a system disturbance occur, e.g. loss of a system infeed/outfeed[1], $P_k$, the resultant system active power imbalance, $\Delta P$, is corrected by a change in the stored rotational energy of the online synchronously-connected masses in the system, $W_{kin,sys}$, and a change in load consumption, $D_{sys}$, due to the frequency deviation, $\Delta f$:

$$\Delta P = \frac{d}{dt} W_{kin,sys} + D_{sys} \Delta f \tag{1}$$

where

$$\frac{d}{dt} W_{kin,sys} \approx \frac{2W^0_{kin,sys}}{f^0} \frac{d}{dt} \Delta f \tag{2}$$

and

$$W^0_{kin,sys} = W^0_{kin,gen} + W^0_{kin,load} = \sum_{\substack{i=1 \\ i \neq k}}^{N} H_i S_i. \tag{3}$$

$W^0_{kin,sys}$ is the total system rotational energy at nominal frequency, $f^0$, and is the sum of the contributions from synchronously-connected generation, $W_{kin,gen}$, and load, $W_{kin,load}$. A machine's inertial constant, $H_i$, and apparent power rating, $S_i$ can be used to compute its stored rotational energy. The *initial* ROCOF, i.e. just after the instance of imbalance, ($0^+ < t \ll t_{gov}$), when $D_{sys}\Delta f \approx 0$, theoretically corresponds to the maximum system ROCOF [16]:

$$\frac{d\Delta f}{dt}\Big|_{t>0^+} = \frac{f^0 P_k}{2\sum_{\substack{i=1 \\ i \neq k}}^{N} H_i S_i}. \tag{4}$$

Two forms of inertial constraint, both with the purpose of mitigating 'insecure' initial ROCOF magnitudes, i.e. ensuring $\left|\frac{d\Delta f}{dt}\Big|_{t>0^+}\right| < \left|\frac{d\Delta f}{dt}\Big|_{max}\right|$, are devised:

1) A static (time-invariant) constraint that ensures the online system stored rotational energy is always above a constant minimum level, defined by the absolute largest infeed/outfeed to the system, $P_{max}$:

$$W^0_{kin,sys} \geq \frac{f^0 P_{max}}{2\left|\frac{d\Delta f}{dt}\Big|_{max}\right|} \tag{5}$$

2) A dynamic constraint that sets the minimum system rotational energy requirement as a function of the largest infeed/outfeed at each UCED time-step, $P_k$:

$$W^0_{kin,sys} \geq \frac{f^0 P_k}{2\left|\frac{d\Delta f}{dt}\Big|_{max}\right|} \tag{6}$$

[1]An infeed is defined as an online generator active power output or HVDC import to the system. An outfeed is defined as an HVDC export from the system.

The dynamic inertial formulation considers the loss of each active power infeed/outfeed, and the post-contingency system inertia following that loss, e.g. if the largest active power output from an online generator is 400 MW, and the largest HVDC import is 500 MW (zero inertial contribution), the constraint determines which contingency will result in the greatest initial ROCOF - which may not necessarily be the loss of the largest infeed. In this example, the loss of the generator may result in a greater post-contingency ROCOF than the loss of the HVDC interconnector, as the system would lose the generator's inertial contribution.

A system's post-disturbance initial ROCOF limit will vary with system size and portfolio capability. In the context of the test system used in this research, the Ireland and Northern Ireland system, a 'secure' initial ROCOF currently equates to $|\text{ROCOF}| \leq 0.5$ Hz/s [11]. This ensures that (i) the ROCOF thresholds of loss of mains protection are not exceeded - mitigating a potentially greater imbalance due to the tripping of distributed generation [19], and (ii) there is sufficient time for a governor response to be fully deployed, so that the frequency nadir/zenith is formed before load/generation shedding thresholds are reached. However, if new ancillary services [6], [7] incentivise investment in emulated inertia or other fast frequency responses, the above 'secure' definition could be redefined, and the inertial constraint reformulated. Due to the difficulty of accurately estimating both the magnitude and temporal nature of $W_{kin,load}$, and to introduce a safety factor into the inertia-constrained UCED, the contribution of load stored rotational energy is not considered here.

### C. Modelling and Test System

The PLEXOS modelling tool [20] and Xpress-MP [21] mixed integer linear programming solver are used to produce daily UCED schedules of the Ireland and Northern Ireland power system [22] at an hourly resolution. Two study years, 2012 and 2020, are considered, due to significantly contrasting levels of installed wind power capacity and HVDC interconnection. The annual energy supplied by wind generation increases from 17% to 37%, and HVDC interconnection between Ireland and Great Britain increases from 500 to 1000 MW. The instantaneous non-synchronous penetration limit, Eq. (7) [10], is 50% and 75% for 2012 and 2020 respectively, as per operational policy forecast [11]. An aggregated (by fuel type) representation of the Great Britain system is used [23]. The model co-optimises the expected costs of system operation and reserve (Table I). The expected costs include variable operation and maintenance, carbon and fuel [24], and start-up cost. In the 2012 model, conventional plant must-run constraints for voltage control in particular network locations are included, as per current operational practice [25]. It is forecasted that such constraints will be relaxed in 2020 due to network reinforcement.

$$\text{Non-Synchronous Penetration} = \frac{P_{wind} + P_{HVDC\,import}}{P_{load} + P_{HVDC\,export}} \tag{7}$$

TABLE I
RESERVE CATEGORIES

| Category | Response Time | Target (% Max. Infeed/Outfeed) | Min. Spinning Requirement (MW) |
|---|---|---|---|
| *Loss of Infeed* | | | |
| Primary | 5 to 15 s | 75 | 160/125† |
| Secondary | 15 to 90 s | 75 | 160/125 |
| Tertiary 1 | 90 s to 5 min | 100 | 160/125 |
| Tertiary 2 | 5 to 20 min | 100 | 160/125 |
| *Loss of Outfeed§* | | | |
| Primary | 5 to 15 s | 100 | 100 |
| *Regulation Reserve* | | | |
| Negative* | n/a | n/a | 150 |

† Lower spinning requirement applies from 00:00-07:00
§ Currently not carried by the system operator
* Sum of the active power headroom above conventional units' min. load

## III. RESULTS

### A. Transition to 'Lighter' AC Synchronous Systems

Hourly UCED schedules were determined for the 2012 and 2020 base case test systems, i.e. no inertial constraint implemented. Fig. 1 is a frequency distribution of the online system stored rotational energy (inertia) in 2012 and 2020. The average wind penetration during the respective periods of online inertia in 2012 and 2020, is also shown. Fig. 1 illustrates that there may be a significant erosion of system inertia due to the displacement of synchronous generation with non-synchronous renewables. For 70% of 2020, the system inertia is below 26.5 GWs - the level required to ensure that the initial ROCOF following the loss of the absolute largest infeed/outfeed, $P_{max}$, does not exceed $\pm 0.5$ Hz/s.

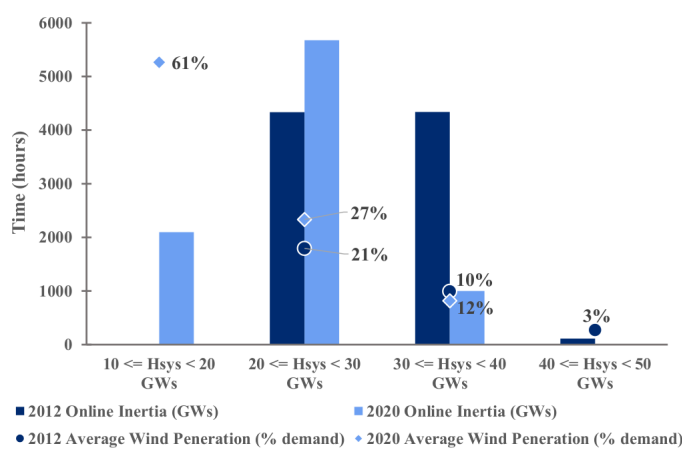


Fig. 1. Frequency distribution of system stored rotational energy (inertia) in 2012 and 2020, with corresponding average wind penetration (% demand)

The implication of 'lighter' synchronous systems is demonstrated in Fig. 2, which shows the initial ROCOF[2] following

[2]All ROCOF plots show the magnitude of the initial ROCOF following the loss of the largest single infeed/outfeed, calculated as per Eq. (4). Thus, the |ROCOF| plotted for each time-step is the greater value that arises from loss of either the largest infeed or the largest outfeed, i.e. the ROCOF plots consider both low (loss of infeed) and high (loss of outfeed) frequency events.

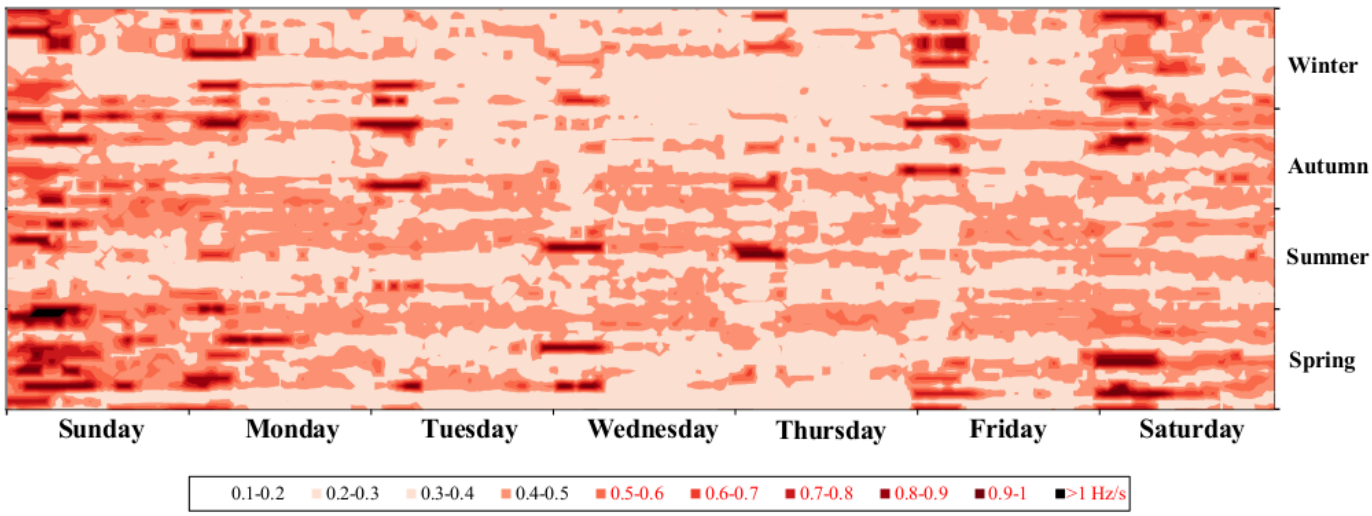


Fig. 2. Heat map showing the initial ROCOF following the loss of the largest single infeed/outfeed online for each hour of 2020 (base case UCED schedule)

loss of the largest single active power infeed/outfeed for each hour of the base case UCED schedule in 2020. While it can be seen that the largest proportion of 'insecure'/high ROCOF (>0.5 Hz/s) periods occur during the weekend (inherently low load periods), there are seasonal variations to the high ROCOF events that occur during the week. Loss of infeed events are the binding contingency for 89.5% of the year, whereas loss of outfeed events account for 10.5%. Fig. 3, a frequency distribution of high initial ROCOF as a function of time of day, shows that, while most extreme ROCOF events (>1 Hz/s) occur during night-time (i.e. 00:00-07:00), there is also a significant variation in the hourly distribution of high ROCOF periods (>0.5 Hz/s) in 2020. Hours which traditionally would not have been associated with frequency instability (e.g. periods of high load), may be prone to high ROCOF; the variable nature of wind generation can result in the decommitment of synchronous plant at any hour in the day. Figs. 2 and 3 highlight that, as wind penetration increases, so too may the operational complexity involved in mitigating high ROCOFs. Furthermore, while Fig. 1 demonstrates that times of high wind generation correspond with those of low online system inertia, this does not necessarily translate to times of 'insecure' ROCOF, as during times of high wind penetration, the largest single infeed may be a conventional unit at its minimum load.

### B. Operational Security Metrics

Operational security metrics reflect operational values showing a strong relationship with relevant system variables. Two such metrics traditionally associated with short-term frequency stability have been (i) the instantaneous wind/non-synchronous penetration level, and (ii) the number of conventional synchronous units online. Fig. 4 shows the relationship between the penetration level of wind generation and the initial ROCOF. Fig. 4 illustrates the relatively uncorrelated nature of wind penetration and initial ROCOF, e.g. with a wind penetration level of 40%, the initial ROCOF can vary from ∼0.2-0.9 Hz/s. This is due to the vast array of operational scenarios experienced for a given wind penetration level. Fig. 5 shows the relationship between the number of 'large' (> 1 GWs of stored rotational energy) conventional synchronous units online and the initial ROCOF. Fig. 5 demonstrates that there can be a significant variation in ROCOF for a given number of large plant online, e.g. with 8 units, the ROCOF can vary from ∼0.25-0.7 Hz/s. Thus, established metrics for frequency stability, such as wind penetration, Fig. 4, and the number of conventional units online, Fig. 5, may not be adequate metrics to predict the initial ROCOF following a generation-load imbalance as non-synchronous penetrations rise. A dedicated inertial policy may be prudent. Such a policy should be based on the level of post-disturbance system inertia and the largest single infeed/outfeed, given the inherent correlation between these variables and the initial ROCOF, Eq. (4).

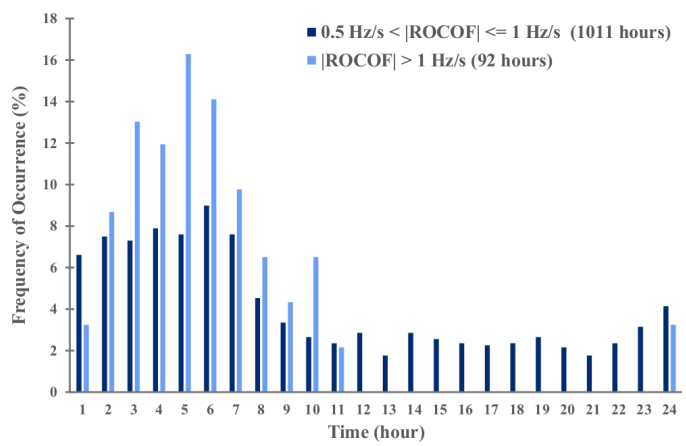


Fig. 3. Frequency distribution of high initial ROCOF as a function of time of day, 2020

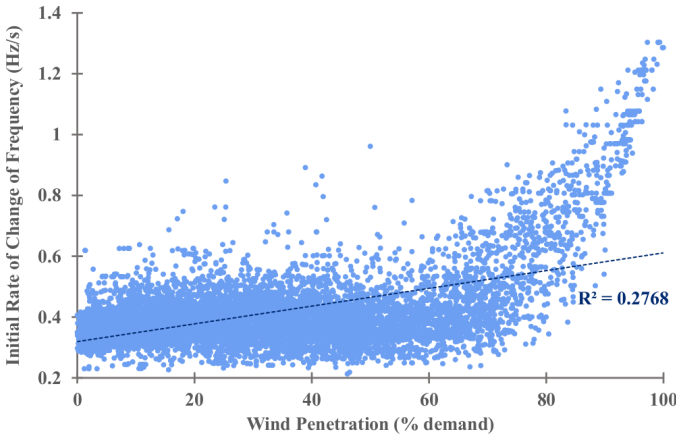


Fig. 4. Initial ROCOF as a function of wind peneration, 2020 base case

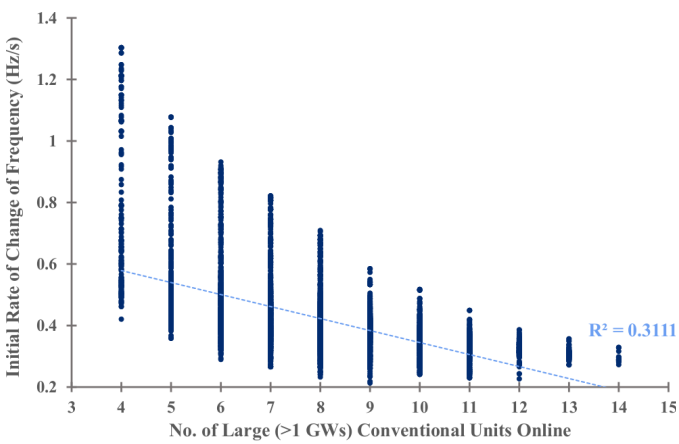


Fig. 5. Initial ROCOF as a function of the number of large conventional units ($>$ 1 GWs stored rotational energy) online, 2020 base case

### C. Inertial Constraint Implementation within UCED

Two forms of inertial constraint (see Section II-B) are incorporated (separately) within UCED, with hourly schedules for 2020 determined. In both cases (static and dynamic), the same initial ROCOF limit of 0.5 Hz/s is maintained, as illustrated by Fig. 6 - a duration curve showing the cumulative probability of the initial ROCOF following loss of the largest single infeed/outfeed for each time-step. As a comparative, a case where a constraint requiring a minimum number of 8 'large' synchronous units online is implemented within UCED, and the 2012 base case, are also shown in Fig. 6. Fig. 6 illustrates that there is little need for an inertial constraint in 2012, due to wind penetrations being significantly lower. Fig. 6 also highlights how a minimum number of units online constraint can be insufficient in mitigating extreme ROCOF. The highest ROCOF magnitudes shown in the base case for 2020 tend to be for loss of the HVDC interconnector at export, during high wind penetrations.

While both static and dynamic inertial constraints attain frequency security (|ROCOF| <0.5 Hz/s), they do so in a contrasting manner. Fig. 7, presented as a duration curve,

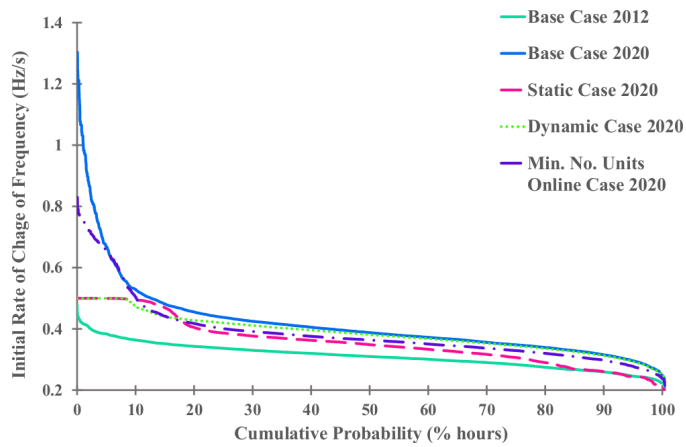


Fig. 6. Duration curve of the initial ROCOF, 2020

shows the difference in (a) the largest single infeed/outfeed, and (b) the number of 'large' synchronous units online, for the base, static and dynamic cases. Fig. 7(a) shows that, with the dynamic constraint implemented, the UCED's optimal solution tends to dispatch down the largest single infeed/outfeed, $P_k$, and increase the output of higher cost plant online, rather than increase the system inertia level, $W^0_{kin,sys}$, and incur the start-up and production costs associated with committing and running out-of-merit synchronous units. The static inertial constraint requires a constant minimum level of inertia - designed to cover the loss of the absolute (time-invariant) largest single infeed/outfeed, $P_{max}$. Consequently, there is a greater number of conventional plant carried online for $\sim$80% of the year with the static target, Fig. 7(b). Fig. 8 contrasts how the static and dynamic constraints alter the UCED schedule for a particular day, showing the difference in (i) the number of large conventional plant online, (ii) the active power output/flow of the largest single infeed and outfeed, and (iii) the level of wind penetration and curtailment, which only occurs in the static case.

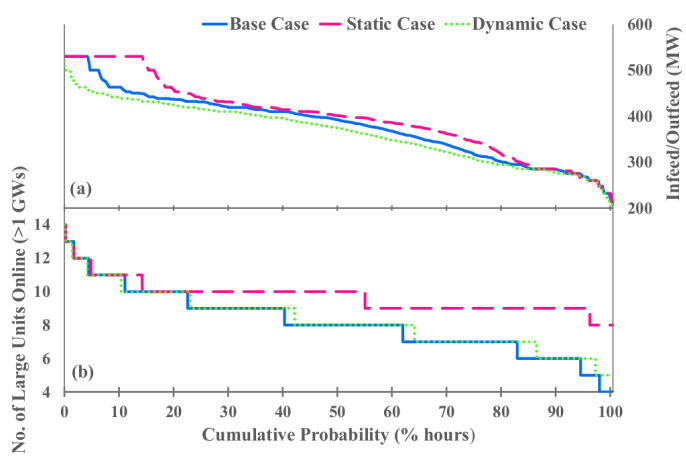


Fig. 7. Duration curve of (a) the largest single infeed/outfeed, and (b) the number of large conventional units online, 2020

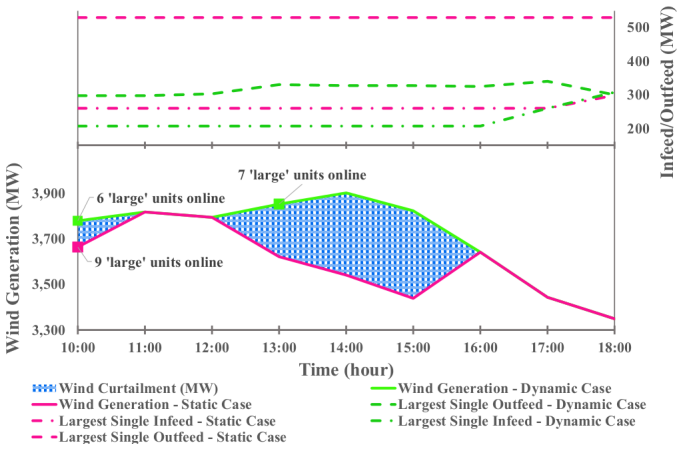


Fig. 8. Comparison of how the dynamic and static inertial constraints alter the UCED schedule: 8 illustrative time-steps, 2020

### D. Total Production Costs and Wind Curtailment

The difference in total production costs and wind curtailment of the UCED schedules are shown in Table II. Comparing the inertial constraint cases, the primary driver of the increase in the total production cost of the static case is the fuel cost associated with the additional number of conventional generators online to meet the time-invariant inertial requirement, Fig. 7(b). Table II highlights that keeping a minimum level of synchronous plant online at all times (for operational security reasons) may have implications for wind curtailment, particularly during low demand/high HVDC import or wind penetration periods. Table II also demonstrates that implementation of a dynamic inertial constraint is a more cost-effective solution for the test system under study, with a total production cost saving of M€10.3 over the static case. With the dynamic constraint committing less synchronous units online, Fig. 7(b), wind curtailment is less than that with the static formulation.

TABLE II
DYNAMIC AND STATIC INERTIAL CONSTRAINT COMPARISON

| Case (2020) | Total Production Costs (M€) | Wind Curtailment (% Energy Available) |
|---|---|---|
| Base | 11,647.99 | 0.5 |
| Dynamic | 11,648.93 | 0.9 |
| Static | 11,659.19 | 2.7 |

## IV. CONCLUSION

As wind, solar and/or HVDC interconnection penetrations grow, the initial ROCOF following large generation-load imbalances may increase significantly - particularly for synchronously isolated systems. Traditional operational metrics, such as the non-synchronous penetration level, and the number of 'large' conventional synchronous units online, may no longer be appropriate proxies for ROCOF, and thus short-term frequency stability as the non-synchronous penetration rises. There may be a need to formulate a specific inertial policy. Two forms of inertial constraint, implemented within UCED, are presented here. It is shown that an inertial constraint that is a function of relevant system variables, such as active power infeeds and outfeeds, and the respective post-disturbance system stored rotational energy level, as opposed to a time-invariant inertial constraint, can reduce both operational costs and wind curtailment.

## REFERENCES


[1] J. Glover, M. Sarma, and T. Overbye, *Power System Analysis and Design*. Cengage Learning, 2011.

[2] S. Sharma, S.-H. Huang, and N. Sarma, "System inertial frequency response estimation and impact of renewable resources in ERCOT interconnection," in *IEEE Power and Energy Society General Meeting*, Detroit, MI, USA, 2011.

[3] D. Gautam, L. Goel, R. Ayyanar, V. Vittal, and T. Harbour, "Control strategy to mitigate the impact of reduced inertia due to doubly fed induction generators on large power systems," *IEEE Trans. Power Syst.*, vol. 26, no. 1, pp. 214–224, Feb 2011.

[4] Y. Wang, V. Silva, and A. Winckels, "Impact of high penetration of wind and PV generation on frequency dynamics in the continental Europe interconnected system," in *13th Wind Integration Workshop*, Berlin, Germany, 2014.

[5] IEA-RETD, "Integration of Variable Renewable Energy. Volume II: Case Studies," Jan. 2015.

[6] ERCOT, "Future Ancillary Services in ERCOT," Sept. 2013.

[7] EirGrid and SONI, "DS3: System Services Review TSO Recommendations," May 2013.

[8] Transpower, "Ancillary Services Procurement Plan," Dec. 2013.

[9] J. Brisebois and N. Aubut, "Wind farm inertia emulation to fulfill Hydro-Québec's specific need," in *IEEE Power and Energy Society General Meeting*, Detroit, MI, USA, 2011.

[10] J. O'Sullivan, A. Rogers, D. Flynn, P. Smith, A. Mullane, and M. O'Malley, "Studying the maximum instantaneous non-synchronous generation in an island system-frequency stability challenges in Ireland," *IEEE Trans. Power Syst.*, vol. 29, no. 6, pp. 2943–2951, Nov 2014.

[11] EirGrid and SONI, "All Island TSO Facilitation of Renewables Studies," June 2010.

[12] P. Cuffe, E. Lannoye, A. Tuohy, and A. Keane, "Unit commitment considering regional synchronous reactive power requirements: costs and effects," in *11th Wind Integration Workshop*, Lisbon, Portugal, 2012.

[13] P. Anderson and A. Fouad, *Power System Control and Stability*. Wiley-Interscience, 2003.

[14] E. Vittal, A. Keane, J. Slootweg, and W. Kling, "Impacts of wind power on power system stability," in *Wind Power in Power Systems*, T. Ackermannn, Ed. Wiley, 2012.

[15] P. Kundur, J. Paserba, V. Ajjarapu, G. Andersson, A. Bose, C. Canizares, N. Hatziargyriou, D. Hill, A. Stankovic, C. Taylor, T. Van Cutsem, and V. Vittal, "Definition and classification of power system stability IEEE/CIGRE joint task force on stability terms and definitions," *IEEE Trans. Power Syst.*, vol. 19, no. 3, pp. 1387–1401, Aug 2004.

[16] M. Chan, R. Dunlop, and F. Scheweppe, "Dynamic equivalents for average system frequency behavior following major disturbances," *IEEE Trans. Power App. Syst.*, vol. PAS-91, no. 4, pp. 1637–1642, July 1972.

[17] G. Lalor, A. Mullane, and M. O'Malley, "Frequency control and wind turbine technologies," *IEEE Trans. Power Syst.*, vol. 20, no. 4, pp. 1905–1913, Nov 2005.

[18] L. Ruttledge, N. Miller, J. O'Sullivan, and D. Flynn, "Frequency response of power systems with variable speed wind turbines," *IEEE Trans. Sustain. Energy*, vol. 3, no. 4, pp. 683–691, Oct. 2012.

[19] R. Walling and N. Miller, "Distributed generation islanding-implications on power system dynamic performance," in *IEEE Power and Energy Society Summer Meeting*, Chicago, IL, USA, 2002.

[20] PLEXOS. [Online]. Available: www.energyexemplar.com

[21] FICO Xpress Opimization Suite. [Online]. Available: www.fico.com

[22] EirGrid and SONI, "All-Island Generation Capacity Statement 2014-2023," Feb. 2014.

[23] National Grid, "Electricity Ten Year Statement," Nov. 2012.

[24] IEA, "World Energy Outlook 2013," Nov. 2013.

[25] EirGrid and SONI, "Operational Constraints." [Online]. Available: http://www.eirgrid.com/aboutus/publications